Fitting the NGC 1560 rotation curve and other galaxies in the 'constant Lagrangian' model for galactic dynamics.

E.P.J. de Haas[1, a)]

Nijmegen, The Netherlands

(Dated: April 24, 2018)

The velocity rotation curve of NGC 1560 has a peculiar wiggle around 4.5 kpc. This makes it a favorable galaxy to test the diverse models trying to explain galactic dynamics, as for example CDM and MOND. I will fit NGC 1560 using the GR-Schwarzschild based 'constant Lagrangian' model for galactic dynamics and compare it to other results. But first I will give a brief expose of the 'constant Lagrangian' approach. At the end, I present same other fitting curves: those of galaxies F583-1, F579V1 and U11648.

PACS numbers: 95.30.Sf, 95.35.+d

Keywords: Dark Matter, MOND, Schwarzschild, Galactic rotation curves

[a)]Electronic mail: haas2u@gmail.com

CONTENTS

I. THE 'CONSTANT LAGRANGIAN' MODEL FOR GALACTIC DYNAMICS

The Lagrangian equation of motion reads

$$\frac{d}{dt}\left(\frac{\partial L}{\partial \dot{q}}\right) - \frac{\partial L}{\partial q} = 0. \tag{1}$$

In classical gravitational dynamics I assume circular orbits with $\dot{q} = v$ and $q = r$. The Lagrangian itself is then given by $L = K - V$, with V the Newtonian potential gravitational energy and K the kinetic energy. One then gets

$$\frac{d}{dt}\left(\frac{\partial L}{\partial \dot{q}}\right) = \frac{dp}{dt} = F. \tag{2}$$

The other part gives

$$\frac{\partial L}{\partial q} = -\frac{dV}{dr}, \tag{3}$$

so one gets Newton's equation of motion in a central field of gravity

$$F_g = -\frac{dV}{dr}. \tag{4}$$

Further analysis of the context results in the identification of the Hamiltonian of the system, $H = K + V$, as being a constant of the orbital motion and the virial theorem as describing a relation between K and V in one single orbit but also between different orbits, $2K + V = 0$.

The previous analysis is problematic relative to the notion of geodetic motion in General Relativity. The problem can best be described in a semi-relativistic approach using the classical Lagrangian equation of motion for geodetic orbits. The most important aspect of geodetic motion in GR is that it requires no force to move on a geodetic. This has important implications for the Lagrangian equation of motion, because $F = 0$ on a geodetic. One gets

$$\frac{d}{dt}\left(\frac{\partial L}{\partial \dot{q}}\right) = F_g = 0 \tag{5}$$

and as a consequence also

$$\frac{\partial L}{\partial q} = -\frac{dL}{dr} = 0. \tag{6}$$

As a result, one gets the crucial

$$L = K - V = constant \tag{7}$$

on geodetic orbits.

This result, the Lagrangian of the system as being the constant of the geodetic motion, is used on a daily basis by many of us because it is used by GNSS systems for the relativistic correction of atomic clocks in their satellites. Let's elaborate this a bit further. If we apply the Schwarzschild metric in polar coordinates, we have (Ruggiero et al., 2008)

$$ds^2 = \left(1 + \frac{2\Phi}{c^2}\right) c^2 dt^2 - \left(1 + \frac{2\Phi}{c^2}\right)^{-1} dr^2 - r^2 d\theta^2 - r^2 sin^2\theta d\phi^2. \tag{8}$$

In case of a clock on a circular geodesic on the equator of a central non-rotating mass M we have $\frac{dr}{dt} = 0$, $\frac{d\theta}{dt} = 0$, $sin\theta = 1$ and $\frac{d\phi}{dt} = \omega$. We thus get, with $v_{orbit} = r\omega$, the GR result

$$\frac{d\tau}{dt} = \sqrt{1 + \frac{2\Phi}{c^2} - \frac{v_{orbit}^2}{c^2}} \tag{9}$$

with $d\tau$ as the clock-rate of a standard clock A in a geodetic orbit and dt as the 'universal' clock-rate G of a standard clock at rest in infinity, the only condition for which $d\tau = dt$. The result of Eqn. (9) is the basic relativistic correction used in GNSS clock frequencies, with the first as the gravity effect or gravitational potential correction and the second as the velocity effect or the correction due to Special Relativity (Ashby, 2002; Hećimović, 2013; Delva and Lodewyck, 2013).

Given the classical definitions of $K = \frac{mv_{orbit}^2}{2}$ and $V = m\Phi$, we get

$$\frac{d\tau}{dt} = \sqrt{1 - \frac{2L}{U_0}}. \tag{10}$$

All the satellites of a GNSS system are being installed on a similar orbit and thus syntonized relative to one another because they share the same high and velocity and have constant L and $\frac{d\tau}{dt}$ on those orbits. But different GNSS systems, as for example GPS compared to GALILEO, are functioning on different orbits with different velocities and those systems aren't syntonized relative to one another. This non-syntonization between satellites on orbits with different heights and virial theorem connected velocities is very annoying for the effort towards realizing an integration of the different GNSS systems into one single global network.

The 'constant Lagrangian' model for galactic dynamics starts with the postulate that the geodetic Lagrangian $L = K - V$ is a galactic constant, not just an orbital constant. In this model the classical Newtonian potential is assumed valid. This potential in the case of a model galaxy with a perfect quasi-solid bulge and a perfect Schwarzschild emptiness around

it is given in Fig.(1). My model galaxy is build of a model bulge with mass M and radius R and a Schwardschild metric emptiness around it. The model bulge has constant density $\rho_0 = \frac{M}{V} = \frac{3M}{4\pi R^3}$ and its composing stars rotate on geodetics in a quasi-solid way. So all those stars in the bulge have equal angular velocity on their geodetic orbits, with $v = \omega r$. On the boundary between the quasi solid spherical bulge and the emptiness outside of it, the orbital velocities are behaving smoothly. So the last star in the bulge and the first star in the Schwarzschild region have equal velocities and potentials. I also assume that the Newtonian potential itself is unchanged and unchallenged, remains classical in the whole galaxy and its surroundings. Such a model galaxy doesn't have a SMBH in the center of its bulge and it only has some very lonely stars in the space outside the bulge.

Point	Relation	Expression
Outside the **bulge**	r > R	$-\frac{GM}{r}$
On the Surface	r = R	$-\frac{GM}{R}$
Inside the **bulge**	r < R	$-GM\left[\frac{3R^2 - r^2}{2R^3}\right]$
At the centre	r = 0	$-\frac{3}{2}\left(\frac{GM}{R}\right)$

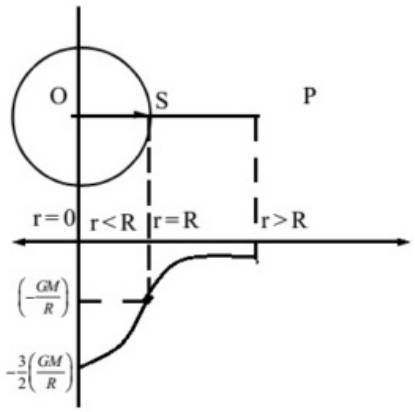

FIG. 1. The potential inside and out of a model bulge

The 'constant Lagrangian model postulates $L = K - V = constant$ in the entire galaxy, without changing the Newtonian potential. As a result, in such a model bulge, L is a

constant of the motion, not only in one orbit but also between orbits.

$$\frac{L}{m} = \frac{v_{orbit}^2}{2} + \frac{GM}{r} = \frac{3GM}{2R} = constant. \tag{11}$$

For the region $0 \leq r \leq R$ we get

$$v_{orbit}^2 = \frac{GM}{R} \cdot \frac{r}{R} \tag{12}$$

and outside the model bulge, where $R \leq r \leq \infty$, we have

$$v_{orbit}^2 = \frac{3GM}{R} - \frac{GM}{r}. \tag{13}$$

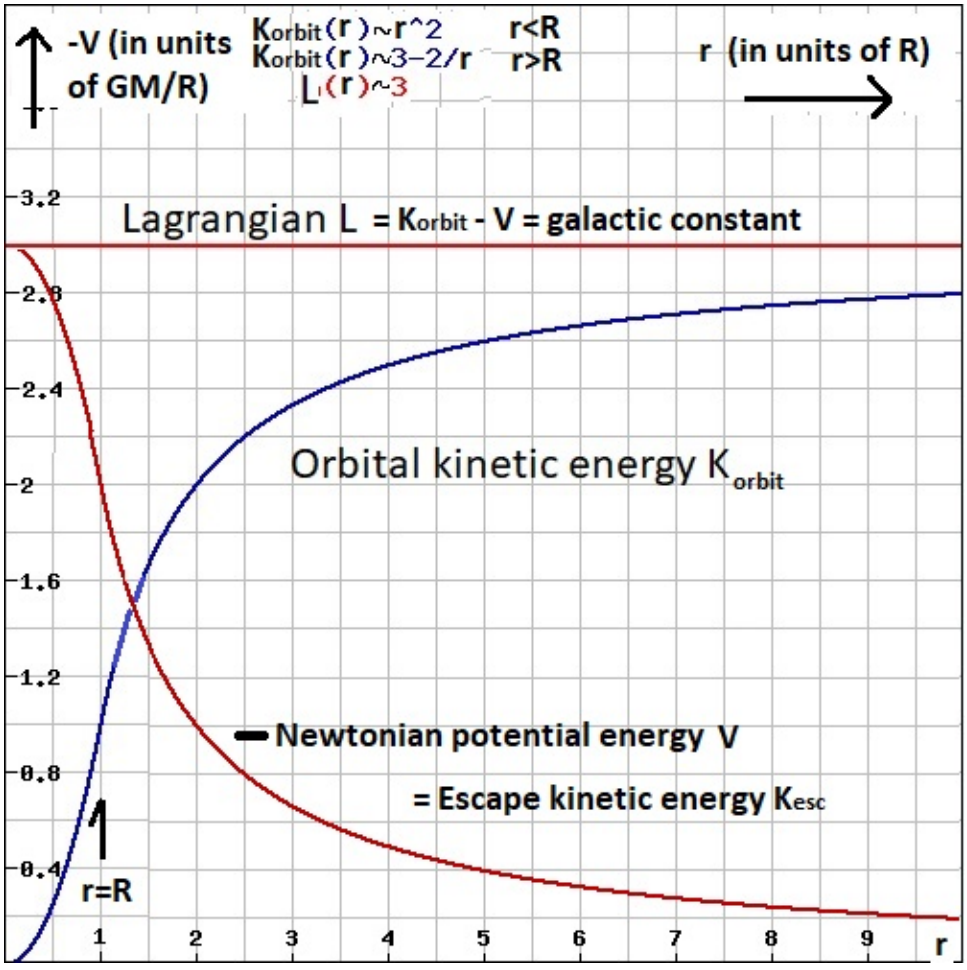

FIG. 2. The square of the orbital velocity profile in the model galaxy with $L = constant$.

From the perspective of a free fall Einstein elevator observer, the free fall on a radial geodetic from infinity towards the center of the bulge, the other free fall tangential geodetics seem to abide the law of conservation of energy, because the escape kinetic energy plus the orbital kinetic energy is a constant on my model galaxy with galactic constant L. An

Einstein elevator system with test mass m that would be put in an orbital collapse situation, magically descending from orbit to orbit in a process in thermodynamic equilibrium, would have constant total kinetic energy, from the radial free fall perspective. This can be expressed as $L = K_{orbit} - V = K_{orbit} + K_{escape} = K_{final}$. In Fig.(2) I sketched the result, with $-V = +K_{escape}$.

Such a model galaxy would also be a GNSS engineer's dream come true because the whole model galaxy is in one single syntonized time-bubble.

$$\frac{d\tau}{dt} = \sqrt{1 - \frac{2L}{U_0}}. \tag{14}$$

Given the Baryonic Tully-Fisher relation in Milgrom's version $v_{final}^4 = Ga_0M$ with $2\pi a_0 \approx cH_0$, with a_0 as Milgrom's galactic minimum acceleration and H_0 as the Hubble constant (Milgrom, 1983; McGaugh, 2005), we get as a galactic time bubble fix

$$\frac{d\tau}{dt} = \sqrt{1 - \frac{2L}{U_0}} = \sqrt{1 - \frac{v_{final}^2}{c^2}} = \sqrt{1 - \sqrt{\frac{v_{final}^4}{c^4}}} = \tag{15}$$

$$\sqrt{1 - \sqrt{\frac{Ga_0M}{c^4}}} = \sqrt{1 - \sqrt{\frac{GH_0M}{2\pi c^3}}} = \sqrt{1 - \sqrt{\frac{M}{2\pi M_U}}}, \tag{16}$$

in which I used $L = 3GM/R = K_{final} = \frac{1}{2}mv_{final}^2$ and $M_U = \frac{c^3}{GH_0}$. This last constant can be referred to as an apparent mass of the Universe, a purely theoretical number constant, see (Mercier, 2015). In a model Universe, this would imply that my model galaxy would be in a proper time bubble with clock-rate $d\tau$ relative to the universal clock-rate dt in proportion to the masses of galaxy M and Universe M_U. In my model galaxy theoretical environment the Baryonic Tully-Fisher relationship implies that the galactic time bubble is fixed through the mass of my model galaxy and that this fix is a cosmological one. So what is a universal acceleration minimum a_0 in MOND can be interpreted as a universally correlated (through M_U) but still local (through M) time bubble fix in my model galaxy geodetic environment. In such a model Universe, the time bubble of a galaxy immediately functions as a gravitational lens, because $\frac{d\tau}{dt}$ as measuring the curvature of the metric also determines the gravitational index of refraction of the time bubble relative to Cosmic space.

II. FITTING THE NGC 1560 ROTATION CURVE

Having determined the model galactic velocity rotation curve based on the Lagrangian as a galactic constant of orbital motion, the question is to what extend real galaxies can be modeled in this way. For this I used the experimental velocity rotation data of galaxy NGC 1560. The velocity rotation curve data come from (Broeils, 1992). The comparison with other fitting models came from (Gentile et al., 2010).

In this section I present the plot of V_{orb}^2 against r, with in each plot the experimental values in red stars and the theoretical values in black bars. The fitting plots are given in two versions. The first plot is with one single fit for M and R, this is the pure model. In the second plot the two parameters M and R are used as one single'free' parameter for every single measurement, because the time-bubble or L is constant constraint leaves only one degree of freedom. The locked in through L variation of M and R in plot 2 can be monitored using the apparent model mass density of the bulge ρ_{bulge}. This density varies as M, with locked in R, varies. With this parameter freedom of one single value, M and with locked R in L and ρ_{bulge}, all four experimental curves could be fitted really nice. The most important cut in the model is the change from the model bulge to the model empty space around it. In the model bulge, $V_{orb}^2 \propto r^2$, outside the model bulge $V_{orb}^2 \propto -r^{-1}$. In the fixed fitting curve, the apparent mass density of the bulge is the main variable that changes due to more realistic circumstances. The excel data sheets of the plots are in the appendix. The fact that it is possible to exactly plot the rotation curves with just one free parameter should be significant for the underlying physics. In my approach, one free parameter can force a time-bubble on a whole galaxy.

But first lets present the results from other approaches, as given in (Gentile et al., 2010). See Fig.(3, 4, 5). In discussing the result, special attention is given to the "wiggle" in the graph and which model can fit it best.

> *In the rotation curve of NGC 1560, as derived by B92, there is a clear "wiggle" in the total rotation velocity, which corresponds very closely to a similar wiggle in the gas contribution to the rotation curve. Mass models such as MOND naturally reproduce the feature, whereas models that include a dominant spherical (or triaxial) halo are too smooth to do so. (Gentile et al., 2010)*

Gentile et. al. conclude that MOND does best and that the success of MOND indicates to

an intimate relation between baryonic mass and galactic rotation curves.

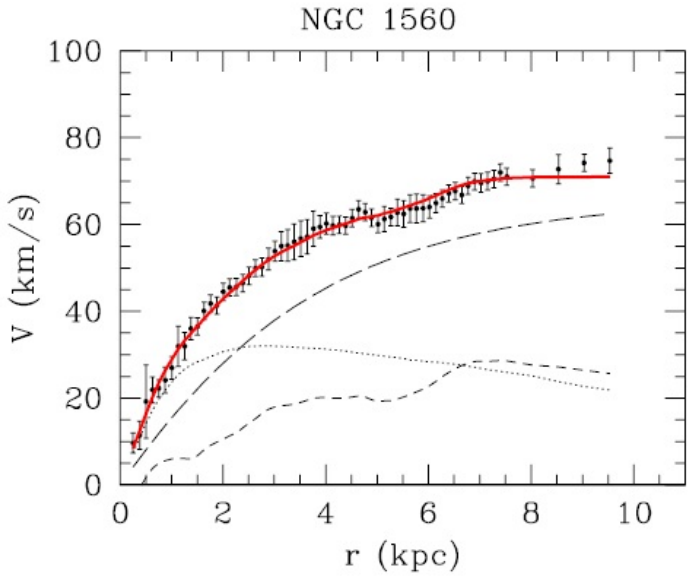

Figure 10. Rotation curve fit using the Burkert halo. Short-dashed, dotted, and long-dashed lines represent the Newtonian contributions of the gaseous disk, stellar disk, and dark halo, respectively. The best-fit model is shown as a solid red line.

FIG. 3. Gentile et. al. fit of NGC 1560, using the Burkert DM distribution.

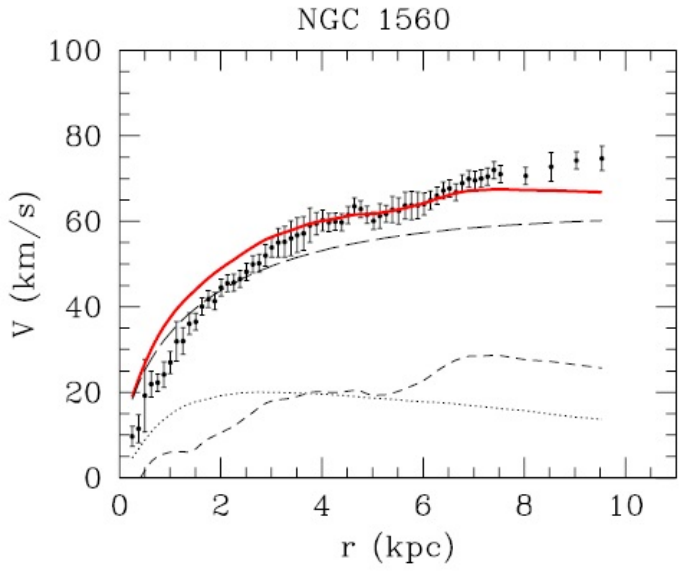

Figure 11. Rotation curve fit using the NFW halo. Lines and symbols are like those in Fig. 10.

FIG. 4. Gentile et. al. fit of NGC 1560, using the NFW DM distribution.

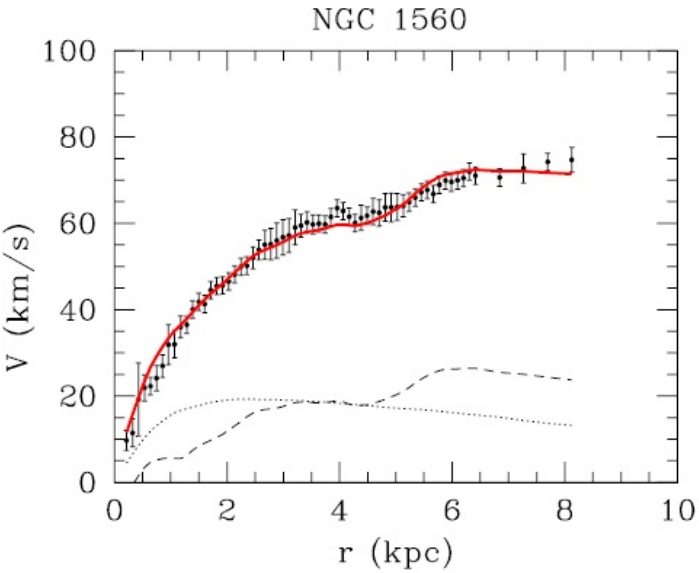

Figure 12. Rotation curve fit using MOND. The best-fit distance is 2.94 Mpc. Lines and symbols are like those in Fig. 10.

FIG. 5. Gentile et. al. fit of NGC 1560, using MOND.

In my approach, I first have to determine the model galaxy that fits best, using the parameters M and R, and then I can use M as a free parameter in order to create a perfect time bubble. In case of NGC 1560 however, its seems that in phase 1 two models partially fit the rotation curve. The first pure model fits NGC 1560 before the "wiggle", see Fig.(6), the second pure model fits NGC 1560 after the "wiggle", see Fig.(7). With the first model, it is almost impossible to then in phase 2 fit the outer range of the velocity curve, while with the second model this is easy. Thus in my approach, the 'constant Lagrangian' model, the modeling indicates the underlying dynamics and the real world of unpredictable mass distributions. The "wiggle" divides NGC 1560 in two regions, which both follow their respective pure model relatively smoothly without being disturbed by that other part of the galaxy. The baryonic matter further away from the center than the H1 gas of producing "wiggle" just behaves as if the bulge end where the "wiggle" ends. The baryonic matter closer to the center than the H1 gas of producing "wiggle" just behaves as if the H1 gas of the "wiggle" is a perfect shell which doesn't gravitate inside that shell. So the fact that two pure models can be made to partially fit the rotation curve actually reveals a lot of the underlying dynamics, reproducing known baryonic behavior.

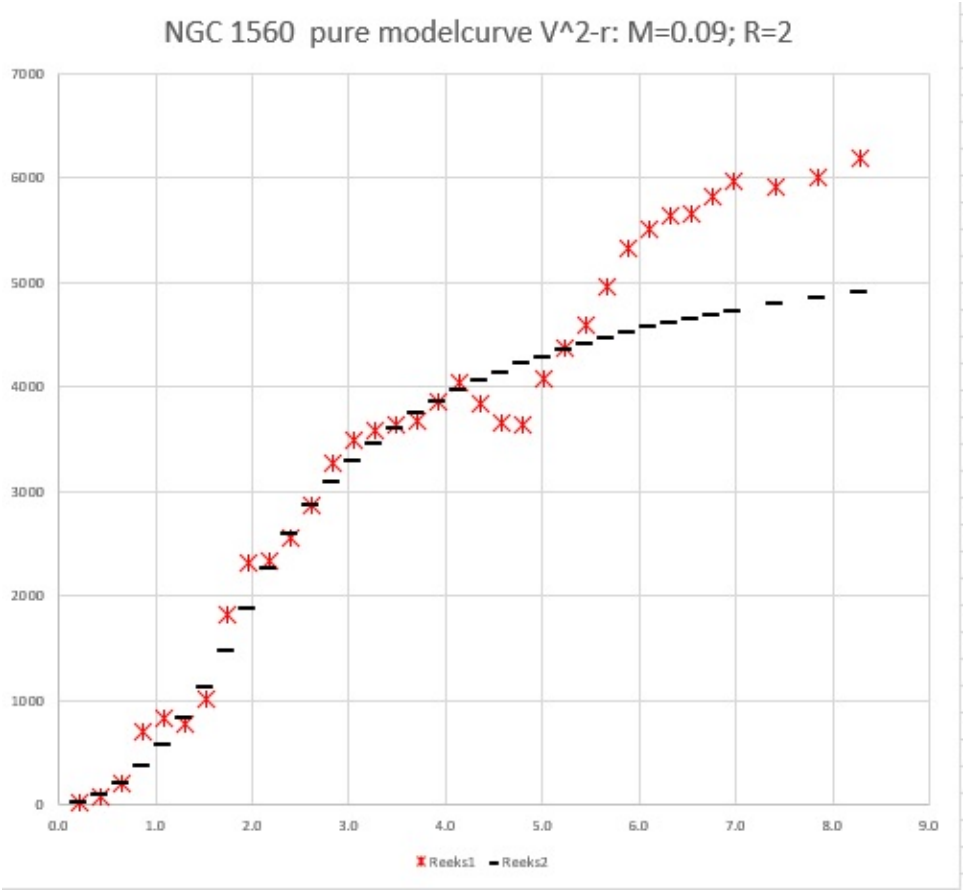

FIG. 6. NGC1560 Plot1, V_{orb}^2 against r, pure model 1 with M=0.09 and R=2.

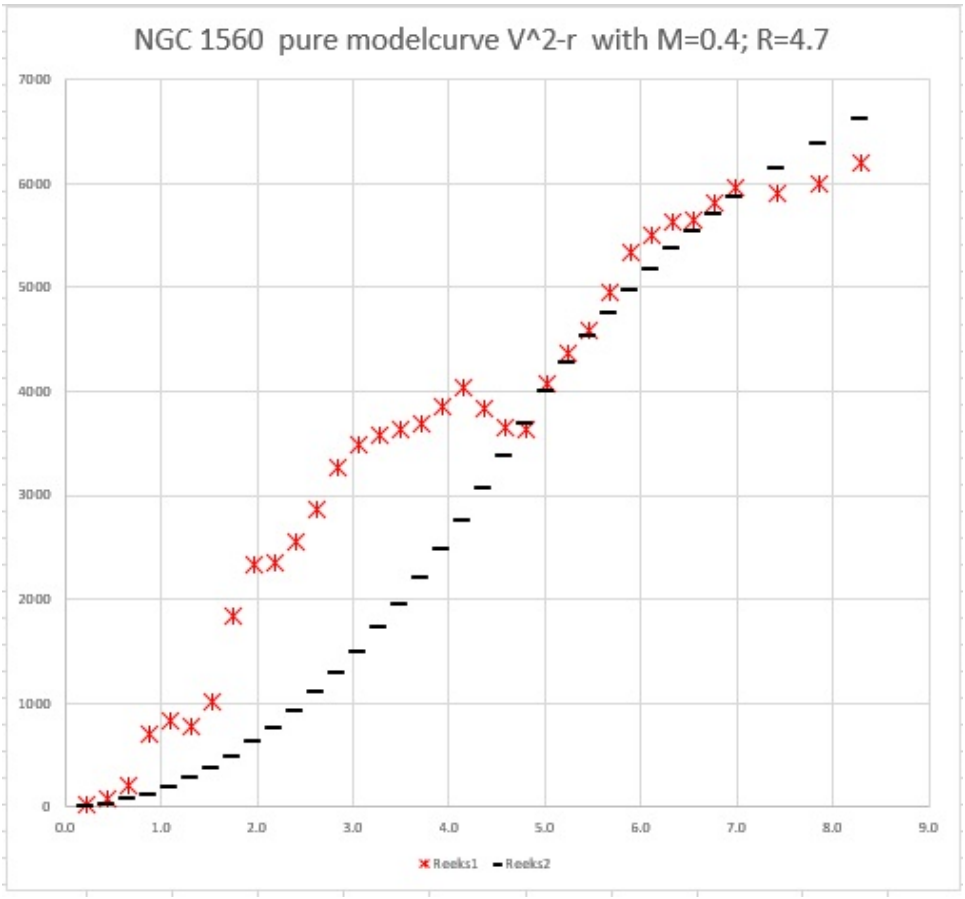

FIG. 7. NGC1560 Plot3, V^2_{orb} against r, pure model 3 with M=0.4 and R=4.7.

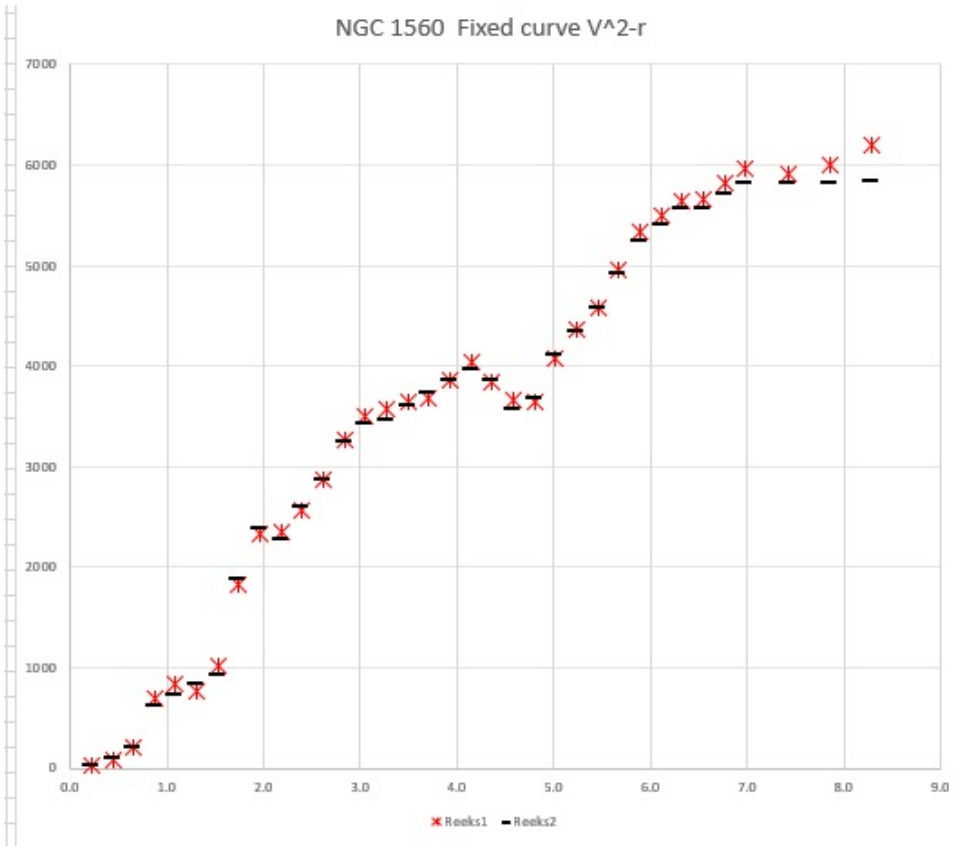

FIG. 8. NGC1560 Plot2, V_{orb}^2 against r, fixed galactic time bubble model of 1. Datasheet in the appendix.

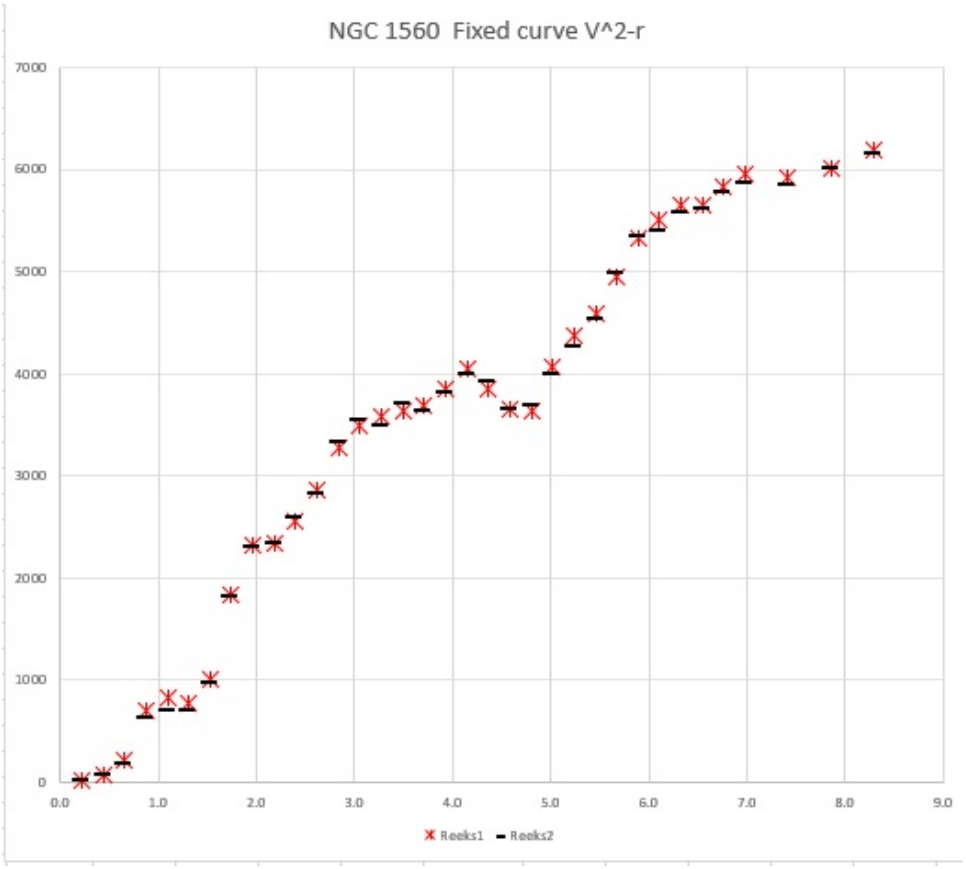

FIG. 9. NGC1560 Plot4, V_{orb}^2 against r, fixed galactic time bubble model of 3. Datasheet in the appendix.

III. SOME MORE ROTATION CURVE FITS: F583-1, F579V1 AND U11648

The data from the following fitting curves are from (McGaugh et al., 2001) and were retrieved from the data website of McGaugh.

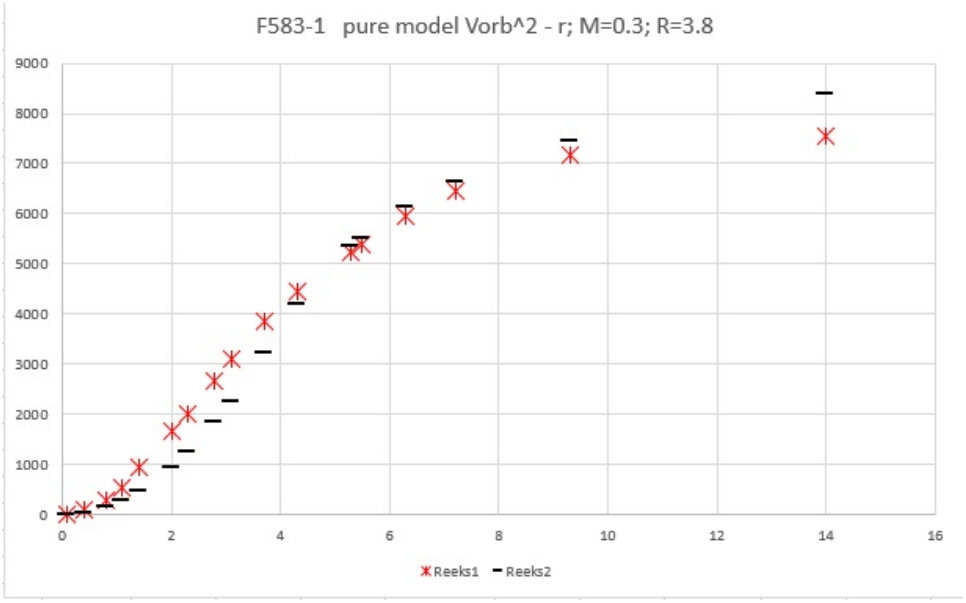

FIG. 10. F583-1 Plot1, V_{orb}^2 against r, pure model 3 with M=0.4 and R=4.7.

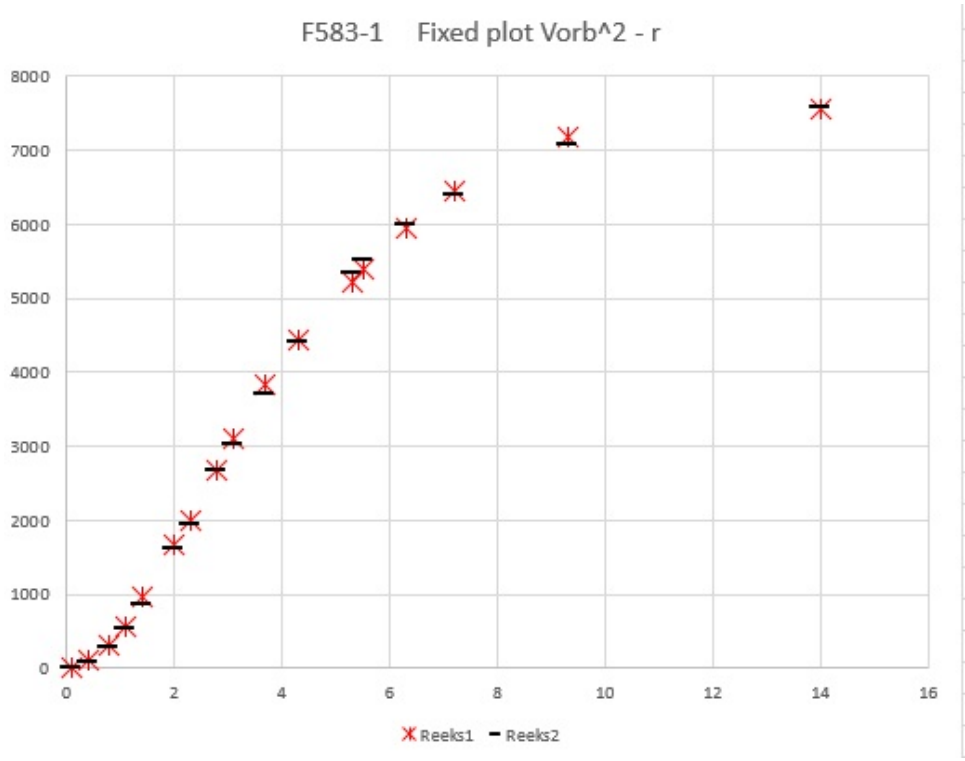

FIG. 11. F583-1 Plot 2, V_{orb}^2 against r, fixed galactic time bubble model of 3. Datasheet in the appendix.

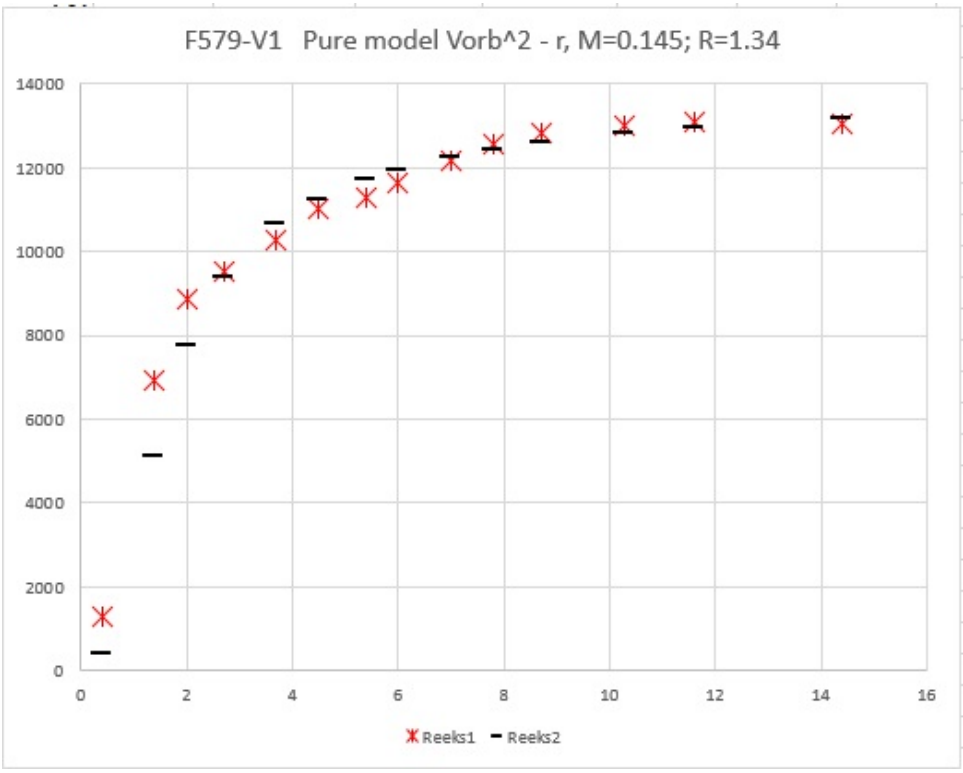

FIG. 12. F579-V1 Plot1, V_{orb}^2 against r, pure model 3 with M=0.145 and R=1.34.

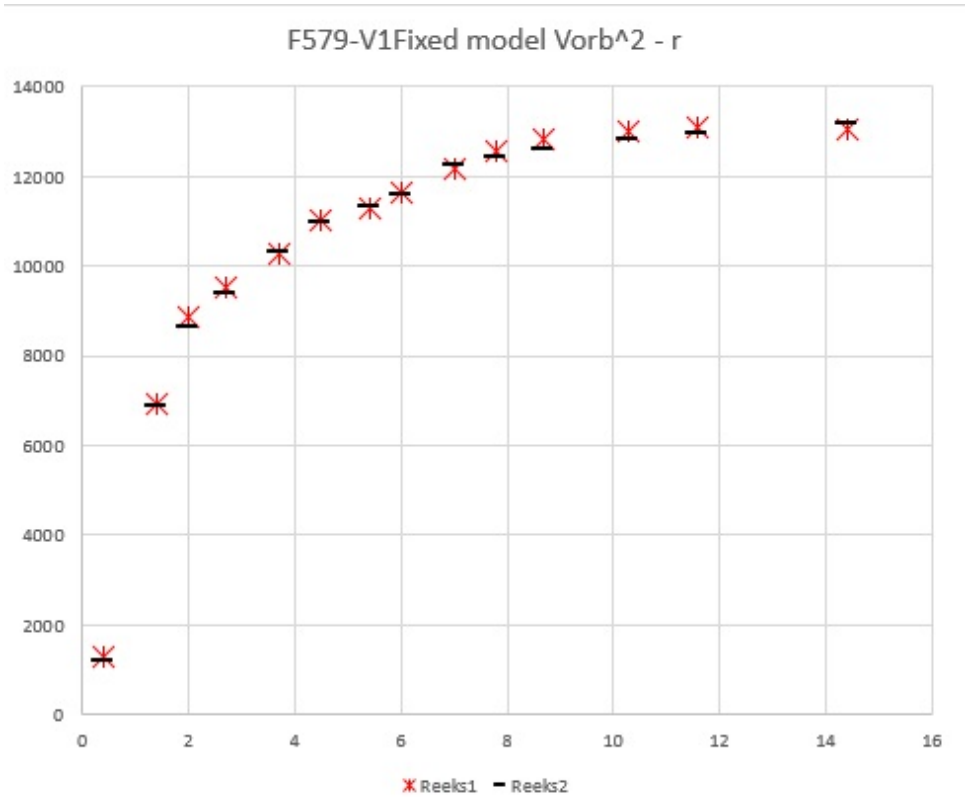

FIG. 13. F579-V1 Plot 2, V_{orb}^2 against r, fixed galactic time bubble model of 3. Datasheet in the appendix.

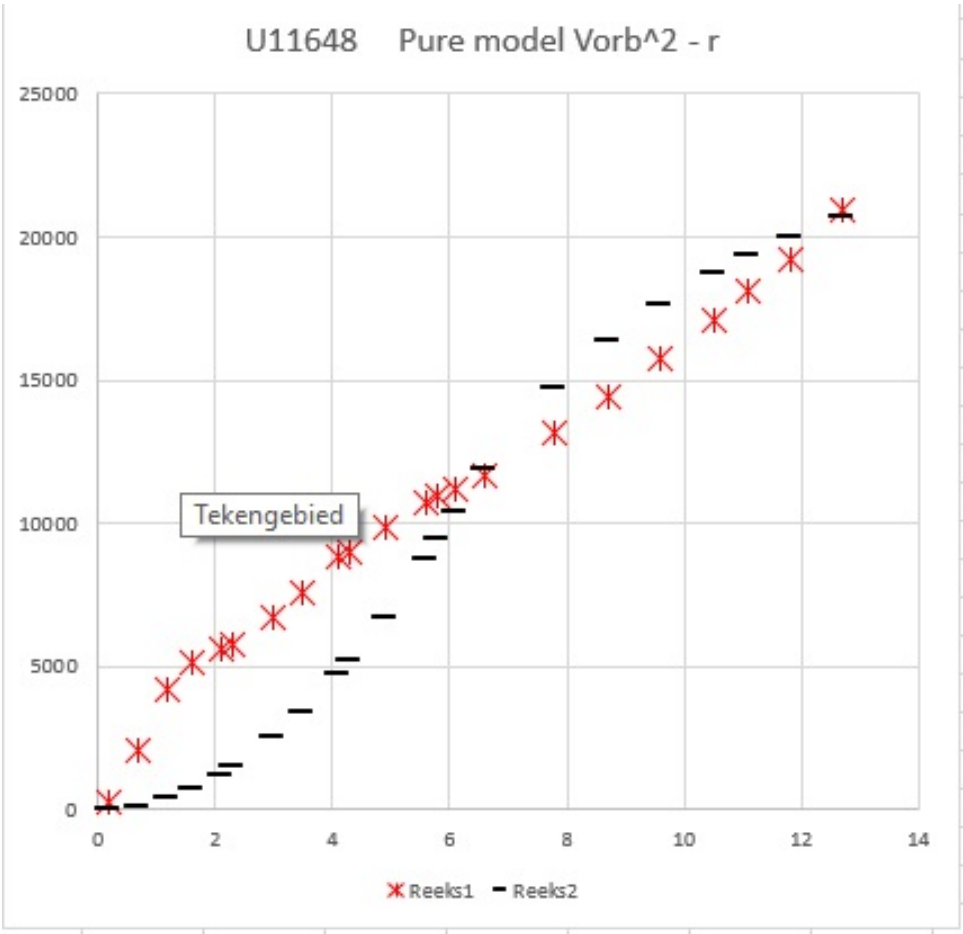

FIG. 14. U11648 Plot 1, V_{orb}^2 against r, pure model 3 with M=0.14 and R=6.

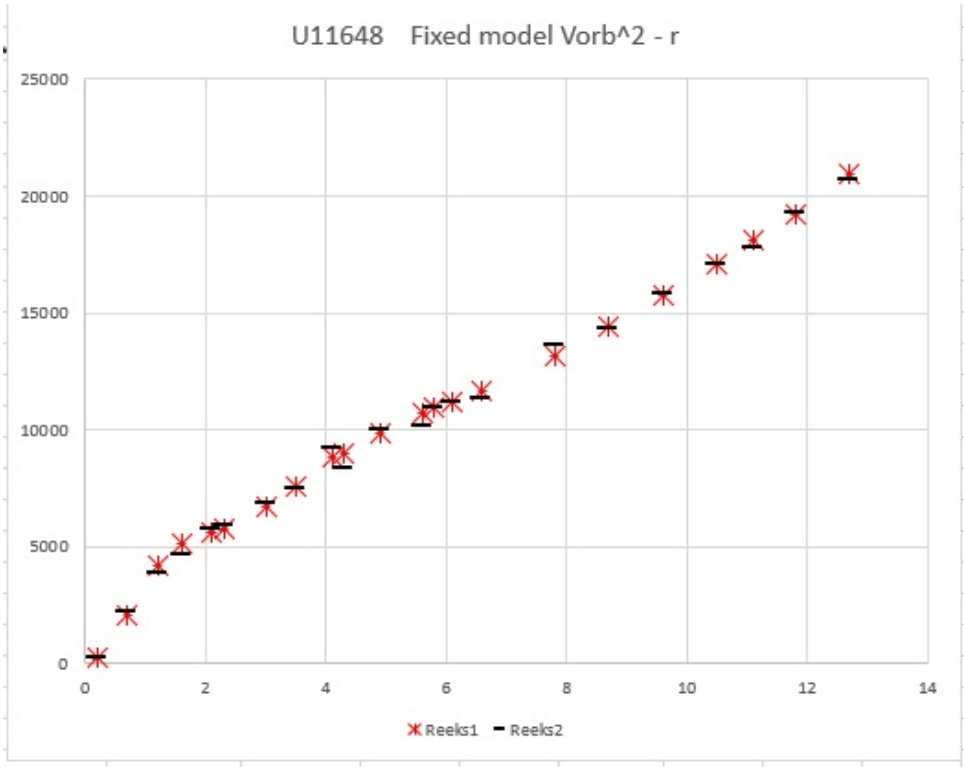

FIG. 15. U11648 Plot 2, V_{orb}^2 against r, fixed galactic time bubble model of 3. Datasheet in the appendix.

REFERENCES

Ashby, N. (2002, May). Relativity and the global positioning system. *Physics Today 55*(5), 41–47.

Broeils, A. H. (1992). The mass distribution of the dwarf spiral ngc 1560. *Astronomy and Astrophysics 256*, 19–32.

Delva, P. and J. Lodewyck (2013). Atomic clocks: new prospects in metrology and geodesy. In *Workshop on Relativistic Positioning Systems and their Scientific Applications Brdo, Slovenia, September 19-21, 2012*. arXiv:1308.6766 [physics.atom-ph].

Gentile, G., M. Baes, B. Famaey, and K. Van Acoleyen (2010). Mass models from high-resolution h i data of the dwarf galaxy ngc 1560. *Monthly Notices of the Royal Astronomical Society 406*(4), 2493–2503.

Hećimović, Ž. (2013). Relativistic effects on satellite navigation. *Tehnički vjesnik 20*(1), 195–203.

McGaugh, S. S. (2005). The baryonic tully-fisher relation of galaxies with extended rotation curves and the stellar mass of rotating galaxies. *The Astrophysical Journal 632*, 859–871. arXiv:astro-ph/0506750v2.

McGaugh, S. S., V. C. Vera C. Rubin, and W. J. G. de Blok (2001). High-resolution rotation curves of low surface brightness galaxies. i. data. *The Astronomical Journal 122*(5), 2381.

Mercier, C. (2015). Calculation of the apparent mass of the universe. Website access (accessed on April, 14, 2018).

Milgrom, M. (1983). A modification of the newtonian dynamics - implications for galaxies. *The Astrophysical Journal 270*, 371–387. Astronomy Abstract Service pdf.

Ruggiero, M. L., D. Bini, A. Geralico, and A. Tartaglia (2008). Emission versus fermi coordinates: applications to relativistic positioning systems. *Classical and Quantum Gravity 25*(20), 205011. arXiv:0809.0998 [gr-qc].

3	R^2 kpc^2	R arcsec	R kpc	Verr pm	V km/s	Vmodel	V (km/s)^2	V^2model	unit GM/R	Mfix	Rfix	fix GM/R	pbulge	3MG/R	Vfinal km/s
	0.05	15	0.2	7.5	5	5	25	23	4.33E+04	0.09	2.0	1.95E+03	2.7	5.84E+03	76
	0.19	30	0.4	9.9	8.9	10	79	93	43253	0.09	2.0	1.95E+03	2.7	5.84E+03	76
	0.43	45	0.7	9.9	14.5	14	210	209	43253	0.09	2.0	1.95E+03	2.7	5.84E+03	76
	0.76	60	0.9	5.6	26.4	25	697	613	43253	0.07	1.6	1.95E+03	4.4	5.84E+03	76
	1.19	75	1.1	5.7	28.9	27	835	733	43253	0.08	1.8	1.95E+03	3.4	5.84E+03	76
	1.71	90	1.3	2.3	27.8	29	773	834	43253	0.09	2.0	1.95E+03	2.7	5.84E+03	76
	2.33	105	1.5	3.2	31.8	30	1011	920	43253	0.1	2.2	1.95E+03	2.2	5.84E+03	76
	3.05	120	1.7	2.1	42.8	43	1832	1877	43253	0.08	1.8	1.95E+03	3.4	5.84E+03	76
	3.86	135	2.0	1.6	48.2	49	2323	2376	43253	0.08	1.8	1.95E+03	3.4	5.84E+03	76
	4.76	150	2.2	1.3	48.4	48	2343	2272	43253	0.09	2.0	1.95E+03	2.7	5.84E+03	76
	5.76	165	2.4	1.0	50.6	51	2560	2596	43253	0.09	2.0	1.95E+03	2.7	5.84E+03	76
	6.86	180	2.6	1.0	53.5	54	2862	2866	43253	0.09	2.0	1.95E+03	2.7	5.84E+03	76
	8.05	195	2.8	1.3	57.2	57	3272	3248	43253	0.085	1.9	1.95E+03	3.0	5.84E+03	76
	9.34	210	3.1	1.5	59.1	59	3493	3433	43253	0.085	1.9	1.95E+03	3.0	5.84E+03	76
	10.72	225	3.3	1.6	59.8	59	3576	3461	43253	0.09	2.0	1.95E+03	2.7	5.84E+03	76
	12.19	240	3.5	1.6	60.3	60	3636	3610	43253	0.09	2.0	1.95E+03	2.7	5.84E+03	76
	13.77	255	3.7	1.6	60.7	61	3684	3741	43253	0.09	2.0	1.95E+03	2.7	5.84E+03	76
	15.43	270	3.9	1.9	62.1	62	3856	3857	43253	0.09	2.0	1.95E+03	2.7	5.84E+03	76
	17.20	285	4.1	1.6	63.6	63	4045	3962	43253	0.09	2.0	1.95E+03	2.7	5.84E+03	76
	19.05	300	4.4	1.6	62	62	3844	3857	43253	0.1	2.2	1.95E+03	2.2	5.84E+03	76
	21.01	315	4.6	1.4	60.5	60	3660	3574	43253	0.12	2.7	1.95E+03	1.5	5.84E+03	76
	23.05	330	4.8	1.5	60.3	61	3636	3677	43253	0.12	2.7	1.95E+03	1.5	5.84E+03	76
	25.20	345	5.0	1.3	63.8	64	4070	4116	43253	0.1	2.2	1.95E+03	2.2	5.84E+03	76
	27.44	360	5.2	1.3	66.1	66	4369	4353	43253	0.09	2.0	1.95E+03	2.7	5.84E+03	76
	29.77	375	5.5	1.2	67.7	68	4583	4571	43253	0.08	1.8	1.95E+03	3.4	5.84E+03	76
	32.20	390	5.7	1.1	70.4	70	4956	4925	43253	0.06	1.3	1.95E+03	6.0	5.84E+03	76
	34.72	405	5.9	1.2	73	72	5329	5252	43253	0.04	0.9	1.95E+03	13.6	5.84E+03	76
	37.34	420	6.1	1.2	74.2	74	5506	5415	43253	0.03	0.7	1.95E+03	24.2	5.84E+03	76
	40.06	435	6.3	1.3	75.1	75	5640	5566	43253	0.02	0.4	1.95E+03	54.4	5.84E+03	76
	42.87	450	6.5	1.2	75.2	75	5655	5575	43253	0.02	0.4	1.95E+03	54.4	5.84E+03	76
	45.78	465	6.8	1.3	76.3	76	5822	5711	43253	0.0100	0.2222	1.95E+03	217.7	5.84E+03	76
	48.78	480	7.0	1.4	77.2	76	5960	5814	43253	0.0020	0.0444	1.95E+03	5441.4	5.84E+03	76
	55.06	510	7.4	1.5	76.9	76	5914	5816	43253	0.0020	0.0444	1.95E+03	5441.4	5.84E+03	76
	61.73	540	7.9	2	77.5	76	6006	5828	43253	0.0010	0.0222	1.95E+03	#####	5.84E+03	76
	68.78	570	8.3	2.3	78.7	76	6194	5838	43253	0.0001	0.0022	1.95E+03	#####	5.84E+03	76

FIG. 16. NGC 1560 Excell datasheet 1, V_{orb}^2 against r, fixed model.

R^2 kpc^2	R arcsec	R kpc	Verr pm	V km/s	Vmodel	V (km/s)^2	V^2model	unit GM/R	Mfix	Rfix	fix GM/R	pbulge	3MG/R	Vfinal km/s
0.05	15	0.2	7.5	5	4	25	20	4.33E+04	0.24	2.9	3.54E+03	2.3	1.06E+04	103
0.19	30	0.4	9.9	8.9	9	79.21	79	43253	0.24	2.9	3.54E+03	2.3	1.06E+04	103
0.43	45	0.7	9.9	14.5	13	210.25	177	43253	0.24	2.9	3.54E+03	2.3	1.06E+04	103
0.76	60	0.9	5.6	26.4	25	696.96	627	43253	0.17	2.1	3.54E+03	4.5	1.06E+04	103
1.19	75	1.1	5.7	28.9	27	835.21	708	43253	0.2	2.4	3.54E+03	3.3	1.06E+04	103
1.71	90	1.3	2.3	27.8	27	772.84	708	43253	0.24	2.9	3.54E+03	2.3	1.06E+04	103
2.33	105	1.5	3.2	31.8	31	1011.24	963	43253	0.24	2.9	3.54E+03	2.3	1.06E+04	103
3.05	120	1.7	2.1	42.8	43	1831.84	1812	43253	0.2	2.4	3.54E+03	3.3	1.06E+04	103
3.86	135	2.0	1.6	48.2	48	2323.24	2293	43253	0.2	2.4	3.54E+03	3.3	1.06E+04	103
4.76	150	2.2	1.3	48.4	48	2342.56	2340	43253	0.22	2.7	3.54E+03	2.7	1.06E+04	103
5.76	165	2.4	1.0	50.6	51	2560.36	2590	43253	0.23	2.8	3.54E+03	2.5	1.06E+04	103
6.86	180	2.6	1.0	53.5	53	2862.25	2831	43253	0.24	2.9	3.54E+03	2.3	1.06E+04	103
8.05	195	2.8	1.3	57.2	58	3271.84	3323	43253	0.24	2.9	3.54E+03	2.3	1.06E+04	103
9.34	210	3.1	1.5	59.1	60	3492.81	3551	43253	0.25	3.1	3.54E+03	2.1	1.06E+04	103
10.72	225	3.3	1.6	59.8	59	3576.04	3495	43253	0.27	3.3	3.54E+03	1.8	1.06E+04	103
12.19	240	3.5	1.6	60.3	61	3636.09	3698	43253	0.28	3.4	3.54E+03	1.7	1.06E+04	103
13.77	255	3.7	1.6	60.7	60	3684.49	3636	43253	0.3	3.7	3.54E+03	1.5	1.06E+04	103
15.43	270	3.9	1.9	62.1	62	3856.41	3818	43253	0.31	3.8	3.54E+03	1.4	1.06E+04	103
17.20	285	4.1	1.6	63.6	63	4044.96	3992	43253	0.32	3.9	3.54E+03	1.3	1.06E+04	103
19.05	300	4.4	1.6	62	63	3844	3918	43253	0.34	4.2	3.54E+03	1.1	1.06E+04	103
21.01	315	4.6	1.4	60.5	60	3660.25	3648	43253	0.37	4.5	3.54E+03	1.0	1.06E+04	103
23.05	330	4.8	1.5	60.3	61	3636.09	3693	43253	0.385	4.7	3.54E+03	0.9	1.06E+04	103
25.20	345	5.0	1.3	63.8	63	4070.44	3994	43253	0.385	4.7	3.54E+03	0.9	1.06E+04	103
27.44	360	5.2	1.3	66.1	65	4369.21	4271	43253	0.385	4.7	3.54E+03	0.9	1.06E+04	103
29.77	375	5.5	1.2	67.7	67	4583.29	4525	43253	0.385	4.7	3.54E+03	0.9	1.06E+04	103
32.20	390	5.7	1.1	70.4	71	4956.16	4989	43253	0.37	4.5	3.54E+03	1.0	1.06E+04	103
34.72	405	5.9	1.2	73	73	5329	5344	43253	0.36	4.4	3.54E+03	1.0	1.06E+04	103
37.34	420	6.1	1.2	74.2	73	5505.64	5392	43253	0.37	4.5	3.54E+03	1.0	1.06E+04	103
40.06	435	6.3	1.3	75.1	75	5640.01	5572	43253	0.37	4.5	3.54E+03	1.0	1.06E+04	103
42.87	450	6.5	1.2	75.2	75	5655.04	5609	43253	0.38	4.6	3.54E+03	0.9	1.06E+04	103
45.78	465	6.8	1.3	76.3	76	5821.69	5771	43253	0.38	4.6	3.54E+03	0.9	1.06E+04	103
48.78	480	7.0	1.4	77.2	77	5959.84	5861	43253	0.385	4.7	3.54E+03	0.9	1.06E+04	103
55.06	510	7.4	1.5	76.9	76	5913.61	5850	43253	0.41	5.0	3.54E+03	0.8	1.06E+04	103
61.73	540	7.9	2	77.5	77	6006.25	6005	43253	0.42	5.1	3.54E+03	0.7	1.06E+04	103
68.78	570	8.3	2.3	78.7	78	6193.69	6144	43253	0.43	5.2	3.54E+03	0.7	1.06E+04	103

FIG. 17. NGC 1560 Excell datasheet 2, V_{orb}^2 against r, fixed model.

R^2 kpc^2	R kpc	V km/s	Vmodel	V (km/s)^2	V^2model	unit GM/R	Mfix	Rfix	fix GM/R	pbulge	3MG/R	Vfinal km/s
0.01	0.1	1.1	2	1	5	4.33E+04	0.2	2.5	3.41E+03	2.94	1.02E+04	101
0.16	0.4	10	9	100	85	43253	0.2	2.5	3.41E+03	2.94	1.02E+04	101
0.64	0.8	17.4	17	303	281	43253	0.22	2.8	3.41E+03	2.43	1.02E+04	101
1.21	1.1	23.5	23	552	532	43253	0.22	2.8	3.41E+03	2.43	1.02E+04	101
1.96	1.4	31	29	961	862	43253	0.22	2.8	3.41E+03	2.43	1.02E+04	101
4.00	2	40.9	40	1673	1609	43253	0.23	2.9	3.41E+03	2.22	1.02E+04	101
5.29	2.3	44.8	44	2007	1955	43253	0.24	3.0	3.41E+03	2.04	1.02E+04	101
7.84	2.8	51.7	52	2673	2670	43253	0.25	3.2	3.41E+03	1.88	1.02E+04	101
9.61	3.1	55.7	55	3102	3026	43253	0.26	3.3	3.41E+03	1.74	1.02E+04	101
13.69	3.7	62	61	3844	3716	43253	0.28	3.5	3.41E+03	1.50	1.02E+04	101
18.49	4.3	66.6	66	4436	4410	43253	0.29	3.7	3.41E+03	1.40	1.02E+04	101
28.09	5.3	72.3	73	5227	5348	43253	0.3	3.8	3.41E+03	1.31	1.02E+04	101
30.25	5.5	73.4	74	5388	5526	43253	0.3	3.8	3.41E+03	1.31	1.02E+04	101
39.69	6.3	77.1	77	5944	5988	43253	0.31	3.9	3.41E+03	1.22	1.02E+04	101
51.84	7.2	80.3	80	6448	6399	43253	0.32	4.1	3.41E+03	1.15	1.02E+04	101
86.49	9.3	84.7	84	7174	7082	43253	0.34	4.3	3.41E+03	1.02	1.02E+04	101
	14	86.9	87	7552	7587	43253	0.43	5.4	3.41E+03	0.64	1.02E+04	101

FIG. 18. F583 1 Excell datasheet 1, V_{orb}^2 against r, fixed model.

R^2 kpc^2	R kpc	V km/s	Vmodel	V (km/s)^2	V^2mode	unit GM/I	Mfix	Rfix	fix GM/R	ρbulge	3MG/R	Vfinal km/s
0.16	0.4	35.7	35	1274	1214	4.33E+04	0.085	0.79	4.68E+03	41.89	1.40E+04	118
1.96	1.4	83.3	83	6939	6875	43253	0.125	1.16	4.68E+03	19.37	1.40E+04	118
4.00	2	94.2	93	8874	8635	43253	0.125	1.16	4.68E+03	19.37	1.40E+04	118
7.29	2.7	97.6	97	9526	9395	43253	0.145	1.34	4.68E+03	14.39	1.40E+04	118
13.69	3.7	101.4	101	10282	10300	43253	0.16	1.48	4.68E+03	11.82	1.40E+04	118
20.25	4.5	105	105	11025	10965	43253	0.16	1.48	4.68E+03	11.82	1.40E+04	118
29.16	5.4	106.2	106	11278	11318	43253	0.17	1.57	4.68E+03	10.47	1.40E+04	118
36.00	6	107.9	108	11642	11590	43253	0.17	1.57	4.68E+03	10.47	1.40E+04	118
49.00	7	110.4	111	12188	12249	43253	0.145	1.34	4.68E+03	14.39	1.40E+04	118
60.84	7.8	112	112	12544	12433	43253	0.145	1.34	4.68E+03	14.39	1.40E+04	118
75.69	8.7	113.2	112	12814	12599	43253	0.145	1.34	4.68E+03	14.39	1.40E+04	118
106.09	10.3	114	113	12996	12823	43253	0.145	1.34	4.68E+03	14.39	1.40E+04	118
134.56	11.6	114.4	114	13087	12960	43253	0.145	1.34	4.68E+03	14.39	1.40E+04	118
207.36	14.4	114.2	115	13042	13170	43253	0.145	1.34	4.68E+03	14.39	1.40E+04	118

FIG. 19. F579 V1 Excell datasheet 1, V_{orb}^2 against r, fixed model.

R^2 kpc^2	Verr^2	R kpc	Verr	V km/s	Vmodel	V (km/s)^2	V^2model	unit GM/R	Mfix	Rfix	fix GM/R	ρbulge	3MG/R	Vfinal km/s
0.04	68	0.2	11.3	16.7	16	279	244	4.33E+04	0.3	1.29	1.01E+04	33.71	3.03E+04	174
0.49	20	0.7	9.1	45.4	47	2061	2198	43253	0.35	1.50	1.01E+04	24.77	3.03E+04	174
1.44	6	1.2	4	64.7	63	4186	3907	43253	0.45	1.93	1.01E+04	14.98	3.03E+04	174
2.56	6	1.6	4.4	71.7	68	5141	4650	43253	0.55	2.36	1.01E+04	10.03	3.03E+04	174
4.41	14	2.1	10.1	74.8	76	5595	5735	43253	0.65	2.79	1.01E+04	7.18	3.03E+04	174
5.29	12	2.3	8.8	75.7	77	5730	5932	43253	0.7	3.00	1.01E+04	6.19	3.03E+04	174
9.00	5	3	4	82	83	6724	6845	43253	0.85	3.64	1.01E+04	4.20	3.03E+04	174
12.25	5	3.5	4	86.9	86	7552	7458	43253	0.95	4.07	1.01E+04	3.36	3.03E+04	174
16.81	6	4.1	5.8	93.9	96	8817	9237	43253	1	4.29	1.01E+04	3.03	3.03E+04	174
18.49	5	4.3	4.6	94.8	92	8987	8397	43253	1.1	4.71	1.01E+04	2.51	3.03E+04	174
24.01	9	4.9	9.3	99.3	100	9860	9976	43253	1.15	4.93	1.01E+04	2.29	3.03E+04	174
31.36	4	5.6	4	103.4	101	10692	10196	43253	1.3	5.57	1.01E+04	1.80	3.03E+04	174
33.64	6	5.8	5.9	104.6	105	10941	10938	43253	1.3	5.57	1.01E+04	1.80	3.03E+04	174
37.21	4	6.1	4	105.7	106	11172	11219	43253	1.35	5.79	1.01E+04	1.66	3.03E+04	174
43.56	6	6.6	6.2	108.1	107	11686	11384	43253	1.45	6.21	1.01E+04	1.44	3.03E+04	174
60.84	4	7.8	4.7	114.7	117	13156	13641	43253	1.5	6.43	1.01E+04	1.35	3.03E+04	174
75.69	3	8.7	4	120.1	120	14424	14368	43253	1.6	6.86	1.01E+04	1.19	3.03E+04	174
92.16	7	9.6	8.2	125.6	126	15775	15860	4.33E+04	1.6	6.86	1.01E+04	1.19	3.03E+04	174
110.25	5	10.5	6.3	130.7	131	17082	17095	43253	1.6	6.86	1.01E+04	1.19	3.03E+04	174
123.21	3	11.1	4	134.7	133	18144	17808	4.33E+04	1.6	6.86	1.01E+04	1.19	3.03E+04	174
139.24	3	11.8	4	138.6	139	19210	19281	43253	1.5	6.43	1.01E+04	1.35	3.03E+04	174
161.29	3	12.7	4	144.6	144	20909	20741	43253	1.4	6.00	1.01E+04	1.55	3.03E+04	174

FIG. 20. U11648 Excell datasheet 1, V_{orb}^2 against r, fixed model.